Spectral Heterogeneity in Protein Fluorescence of Bacteriorhodopsin: Evidence for Intraprotein Aqueous Regions†

Balbina J. Plotkin and Warren V. Sherman*

ABSTRACT: By the use of derivative spectral analysis, the broad tryptophan (Trp) fluorescence emission from aqueous suspensions of bacteriorhodopsin in its native purple membrane may be resolved into contributions from buried, surface, and exposed residues. Addition of glycerol produces a progressive enhancement of the fluorescence yield to a limiting value at about 70% v/v glycerol. Glycerol enhancement of fluorescence is also observed for monomeric Trp, and a good correlation exists between this effect and literature estimates of the fractional degree of Trp exposure in nine globular proteins. The estimate of fractional Trp exposure in bacteriorhodopsin from this correlation (50 ± 15%) is in agreement with the value obtained by spectral differentiation and also by modified Stern–Volmer curves for quenching by water-soluble acrylamide. The absence of significant quenching by Tb(III) or Eu(III) ions, which may be expected to bind to the purple membrane surface, shows that the exposed Trp residues are in contact with water in intraprotein regions of the membrane and may be the first direct evidence for a transmembrane aqueous channel by which protons are actively transported during the bacteriorhodopsin photochemical cycle.

Bacteriorhodopsin (BR),[1] the photoresponsive protein of the purple membrane of halophilic bacteria, has been widely studied as a model light-transducing system and as an analogue of the mammalian visual pigment [for recent reviews, see Stoeckenius & Bogomolni (1982)]. BR consists of a simple polypeptide of 248 amino acids (Khorana et al., 1979; Ovchinnikov et al., 1979) with a retinylidene chromophore attached via a protonated aldimine bond at Lys-216 (Bayley et al., 1981; Oesterhelt et al., 1981; Huang et al., 1982). The polypeptide chain is folded into 7 helical segments, each of about 30 residues, which span the membrane (Henderson & Unwin, 1976; Blaurock, 1976). Labeling the helical segments A–G sequentially along the polypeptide chain starting at the amino terminus (Figure 1A), it has been suggested that some of the nonhelical linking sections are of sufficient length that neighboring segments in the membrane are not necessarily in alphabetical order (Engelman et al., 1981). Thus, identification of the protein helical segments with membrane sites obtained from X-ray and electron diffraction density maps (Figure 1B) is a nontrivial task. One of us has addressed this question previously (Sherman, 1982) and suggested that the number of possibilities could be narrowed down to three or four of the nine best models of Engelman et al. (1980). [Another of these best models was selected, however, by Stoeckenius & Bogomolni (1982).]

The mechanism of ion translocation is central to the complete understanding of structure–function relationships in the purple membrane and also, by extrapolation, in mammalian visual pigments. BR provides a light-energized unidirectional flow of protons across the bacterial cell membrane. The chronology of this proton pump has been related to spectrally identified transients that make up the photocycle [see Ottolenghi (1980) and references cited therein]. A gate must be present to prevent the reversal of the light-driven proton flux (Stoeckenius et al., 1979), but no gross conformational change in the protein has been detected (Honig, 1982). The possiblity of an aqueous channel traversing animal rhodopsin in the rod outer section membrane has been suggested (Downer & Englander, 1977; Montal et al., 1977), and there is evidence for hydrophilic regions within the interior of the purple membrane containing the bacterial analogue BR (Rogan & Zaccai, 1981) and the involvement of water at the retinylidene binding site of BR [see Korenstein & Hess (1982) and references cited therein]. In this paper, results will be presented which demonstrate the existence of aqueous regions within the BR protein matrix and thus support the putative channel theory for ion translocation.

Materials and Methods

Materials. Halobacterium halobium M1 was grown by using standard methods as described previously (Sherman et al., 1975) with minor differences. The latter includes using casamino acids (Difco, Detroit, MI) as the primary nutrient and aeration during the initial growth phase by air bubbling rather than shaking in open vessels. Isolation and purification of purple membrane (PM) containing BR were as described previously. PM was separated from brown membrane at the sucrose gradient stage (Oesterhelt & Stoeckenius, 1974). Samples were kept for subsequent use either under refrigeration in aqueous phosphate buffer (pH 7) or, after lyophilization, as a dry powder stored in a vacuum desiccator at room temperature. The apomembrane, containing bacterioopsin (BO) and membrane-bound retinal oxime, was produced by illuminating an aqueous PM suspension at pH 8–9 with light filtered through aqueous dichromate in the presence of hydroxylamine according to the method of Becher & Cassim (1975). Retinylidene-free BO was prepared by the method of Tokunaga & Ebrey (1978) by extracting freeze-dried apomembrane with petroleum ether (Fisher, bp 30–60 °C) to remove membrane-bound retinal oxime. The product, upon resuspension in aqueous buffer, exhibited no absorption bands at wavelengths longer than that of the protein (γ) band other than a small band at ca. 550 nm at the instrumental detection limit (Cary Model 118C) corresponding to the α-band of BR.

† From the Department of Physical Sciences, Chicago State University, Chicago, Illinois 60628. *Received November 22, 1983.* This work was supported by National Institutes of Health Grants R01-02219 and RR08043 and National Science Foundation Grant PRM 8303454.

[1] Abbreviations: BR, bacteriorhodopsin; BO, retinylidene-free bacterioopsin; PM, purple membrane; Trp, tryptophan; Tyr, tyrosine; Arg, arginine; Asp, aspartic acid; Glu, glutamic acid; NATA, *N*-acetyltryptophanamide; LADH, horse liver alcohol dehydrogenase; Tris, tris(hydroxymethyl)aminomethane.

0006-2960/84/0423-5353$01.50/0

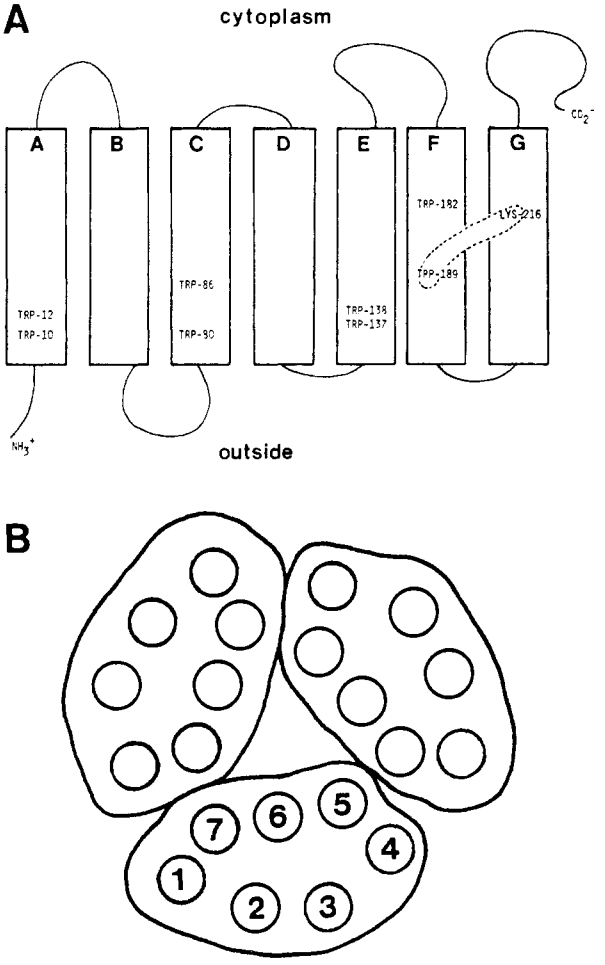

FIGURE 1: (A) Polypeptide chain of bacteriorhodopsin in the native purple membrane showing the approximate locations of Trp residues in seven helical segments on the basis of Huang et al. (1982). (B) Approximate lateral locations of the seven helical segments of trimeric BR in the native purple membrane at −5 Å from the membrane center [after Henderson (1975)]. The numbering of the helical section positions is that of Engelman et al. (1980) and is viewed from the cytoplasmic side.

N-Acetyltryptophanamide (NATA), L-tryptophan, and the proteins used in the glycerol-perturbation study were used as received (Sigma).

Fluorometry. Fluorescence spectra were obtained with a Perkin-Elmer Model 650-40 spectrofluorometer. Data storage and manipulation were performed with a Perkin-Elmer Model 3600 data station microprocessor. Emission spectra are all corrected for solvent Raman scattering but not corrected for instrumental factors. A corrected spectrum of aqueous monomeric Trp was obtained by using a rhodamine B quantum counter. Comparison of this spectrum with an uncorrected scan of the same solution showed that ordinate distortion was less than 3% over the spectral range 320–380 nm. Samples were prepared by diluting stock lipoprotein suspensions such that the final 280-nm absorbance was in the range 0.05–0.10. On the basis of an apparent extinction coefficient of 9.3×10^4 M^{-1} cm^{-1} (this includes a contribution due to light scattering; Becher et al., 1978), the BR concentrations in aqueous PM suspensions were thus 0.54–1.1 μM. Unless otherwise noted, the suspending aqueous medium contained either Tris (Sigma) or phosphate (Fisher) buffer (0.05 M). Absorption spectrophotometry was performed with a Cary Model 118C instrument with the cuvette positioned alongside the photodetector window to minimize scattering. PM samples were adapted to normal room illumination prior to measurement. The fluorometer cuvette holder was maintained at 20 °C by means of a circulating water bath, and unless otherwise noted, the band-pass on both excitation and emission monochromators was 2 nm. All fluorescence intensities measured in the presence of quenchers are corrected for absorption of excitation light by the quencher at the wavelength used.

To enhance spectral heterogeneity, spectra stored on magnetic disks were reprocessed electronically to obtain *n*th-order derivative spectra [Savitsky & Golay, 1964; see O'Haver & Green (1976) and references cited therein; Cahill, 1979] using a BASIC listing by J. F. Williams (1981). A finite wavelength interval for differentiation of 10 nm was used throughout as optimal for maximizing the signal and suppressing the artifacts due to noise in the integral spectrum.

Table I: Comparison of Protein Fluorescence Spectra and Yields

fluoro-phore	λ_{max} (nm)	$\Delta\lambda$ (nm)	rel lumines-cence[a]	rel quantum yield[b]	quantum yield[c]
BR	327	66	1.0	1.0	0.015
BO	333	60	5.8	5.2	0.077
BO + retinal oxime	329	60	0.56	1.6	0.024
Trp	356	64	14.0	9.3	0.135

[a] 280-nm excitation. All samples with identical 280-nm optical density. [b] Corrected for contribution of Tyr and retinylidene to the 280-nm absorbance. [c] Based on tryptophan in water with a quantum yield of 0.135.

Results

Protein Emission. Fluorescence emission parameters for the three aqueous lipoprotein suspensions, BR, BO, and light-bleached BR (BO + retinal oxime), together with monomolecular Trp are listed in Table I. The excitation wavelength was 280 nm, and for the purpose of comparing quantum yields, all solutions were prepared such that their 280-nm absorbances were identical. Relative quantum yields were calculated by comparing the areas under the emission bands (by weighing) with that of Trp after correction was made for the contribution to the 280-nm absorption for each protein from Tyr (assumng, respectively, 11 and 8 Tyr and Trp residues per protein molecule) by using hydrophobic extinction coefficients for Tyr and Trp estimated by Donovan (1969) and also for retinyl absorbance (Becher et al., 1978).

Variability in BO quantum yield has been noted previously (Sherman, 1982). This was attributed to quenching by residual retinal oxime and also incomplete bleaching of the chromophore. The present value (Table I) is that of our "best" samples (N = 6; SD = 7%) in which no detectable visible absorption band was present after light bleaching in the presence of hydroxylamine and in which solvent extraction of retinal oxime was continued to constant absorbance in the 350-nm region.

All the lipoprotein suspensions exhibited similar excitation spectra with a maximum at 284 nm and a shoulder at ca. 290 nm. Those for BR are shown in Figure 2. Excitation spectra for aqueous monomolecular Tyr and for Trp in water, in dioxane–water mixtures, and in 2-propanol were also measured and are included in Figure 2. It may be seen that the lipoprotein excitation spectrum closely resembles that for Trp in organic solvents. To separate possible contributions from Tyr to the overall protein emission, comparison was made between the 340-nm emmision for 280- and 295-nm excitation. For the latter excitation, no contribution from Tyr residues may be expected in proteins. The results are summarized in Table II.

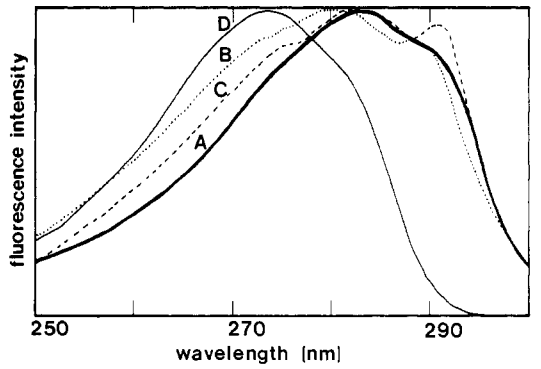

FIGURE 2: Excitation spectra (normalized) for 340-nm emission: (A) bacteriorhodopsin (BR); (B) tryptophan in water (pH 7); (C) tryptophan in 2-propanol; (D) tyrosine in water (pH 7, 305-nm emission).

Table II: Environmental Effects on Excitation Wavelength Dependence of Trp Fluorescence Emission

fluorophore	dielectric constant[a]	I_{280}/I_{295}
NATA in water	80	2.9
NATA in 50% dioxane	67	2.0
NATA in 90% dioxane	29	2.0
NATA in dioxane	2.2	1.7
NATA in 2-propanol	18	1.9
BR		2.2
BO		2.0

[a] Calculated on the basis of the dielectric constant of mixture = $\sum D_i X_i$ where D_i and X_i are respectively the dielectric constant and the mole fraction of the ith component of the mixture. Dielectric constants are taken from the *Handbook of Physics and Chemistry* (1980).

Table III: Tryptophanyl Emission Spectral Heterogeneity[a]

fluorophore[b]	rel signal amplitude (%) at nominal wavelength maxima[c] 325	340	360	rel amplitude of exposed Trp, I_R[d]
BR	51	18	31	0.45
BO	54	18	28	0.39
BO + retinal oxime	52	22	26	0.35
LADH	65	5	30	0.43
NATA	35		65[e]	1.9[e]
NATA + 2-propanol	52	19	29	0.41
NATA + 50% (v/v) aqueous dioxane	50	24	28	0.39
NATA + 90% (v/v) aqueous dioxane	54	19	23	0.37
NATA + dioxane	59	20	21	0.26

[a] From fourth-derivative spectra. [b] In aqueous suspension, pH 7, unless stated otherwise. [c] Wavelength in nanometers. [d] $I_R = I_{360}/(I_{325} + I_{340})$. [e] Broad unresolved band with maxima at ca. 350 and 362 nm. Relative signals based on band areas.

Derivative spectroscopic techniques [see O'Haver & Green (1976) and references cited therein; Butler, 1979; Cahill, 1979] were used to enhance the resolution of the putative overlapping Trp fluorescence emission bands for the aqueous lipoprotein suspensions listed in Table I. The results for BR and BO are shown in Figure 3. It may be seen that for both membrane-bound proteins, the pseudomonotonic integral emission spectrum (Figure 3A) is partly resolved in the second-derivative spectrum (Figure 3B) into two bands with maxima at ca. 325 and 360 nm (exhibited as minima) with the shorter wavelength bands in both proteins showing a shoulder on their long-wavelength edge. The latter is resolved in the fourth derivative (Figure 3C) into a band at ca. 340 nm. The relative intensities of these bands are listed in the second through fourth columns of Table III, and the last column lists the ratio (I_R) of the emission intensity attributable to exposed Trp residues (emission maximum ca. 360 nm) relative to the sum of the

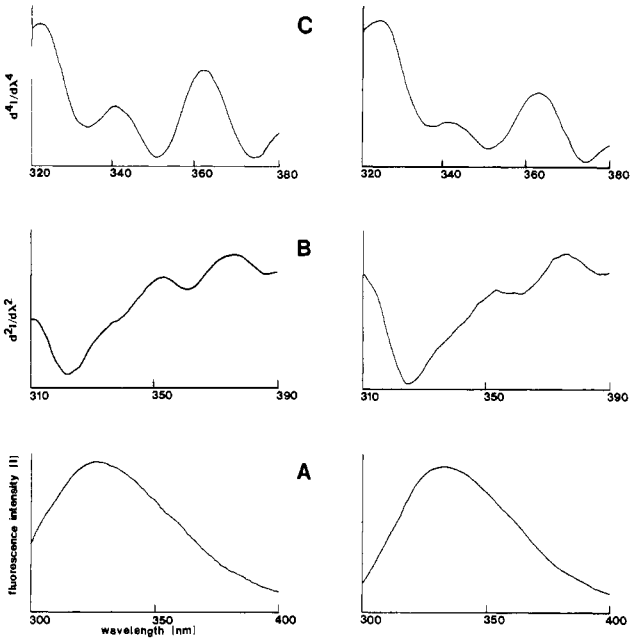

FIGURE 3: Resolution of heterogeneity in the fluorescence emission band of native bacteriorhodopsin (left-hand spectra) and retinylidene-free bacterioopsin (right-hand spectra): (A) emission spectra; (B) second-derivative spectra; (C) fourth-derivative spectra. Excitation wavelength, 280 nm; emission and excitation bandwidths, 2 nm; derivative calculations are with respect to wavelength increments ($\Delta\lambda$) of 10 nm.

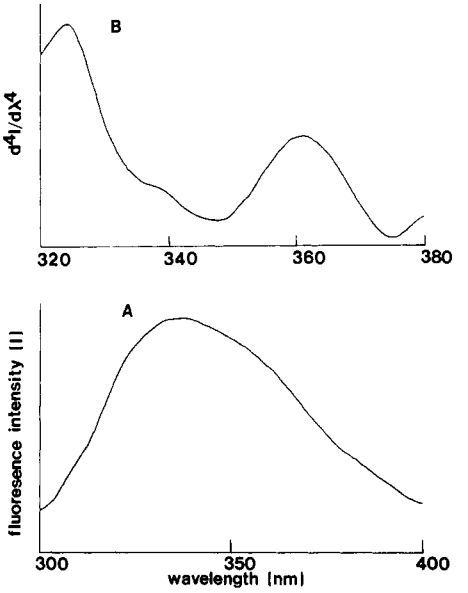

FIGURE 4: Fluorescence emission spectra of horse liver alcohol dehydrogenase (LADH): (A) fluorescence intensity (I) vs. wavelength (λ); (B) $d^4I/d\lambda^4$ vs. λ, 295-nm excitation.

intensities of the other two bands. For comparison, results for horse liver alcohol dehydrogenase (LADH) and also NATA in water, dioxane–water mixtures and 2-propanol are included in this compilation. The emission spectrum of LADH is shown in Figure 4 (295-nm excitation).

Solvent Perturbation Fluorometry. A progressive enhancement of fluorescence quantum yield for both BR and BO was observed in the presence of increasing concentrations of glycerol, reaching limiting values for 295-nm excitation of 60% and 40%, respectively, at ca. 70% v/v glycerol. There was no detectable change (±2 nm) in the emission maxima for both proteins, and the magnitude of the enhancement was excitation wavelength dependent (greater for 295-nm than for 280-nm

Table IV: Correlation between the Enhancement of Protein Fluorescence Yield by Glycerol and Trp Exposure

protein[a]	F_g/F_w[b]	exposed Trp (%)	ref
(1) arginase	1.0	0	Burstein et al. (1973)
(2) BO	1.4		
(3) BR	1.7		
(4) chymotrypsin	1.4	0	Burstein et al. (1973)
(5) HSA	1.2	0	Bell & Brenner (1982)
(6) LADH	1.7	50	Ross et al. (1981)
(7) lysozyme	1.7	50	Rousslang et al. (1979)
(8) NATA	2.2	100	
(9) papain	1.6	67	Burstein et al. (1973)
(10) pepsin	1.4	40	Burstein et al. (1973)
(11) subtilisin C	2.3	100	Longworth (1971)
(12) trypsin	1.5	0	Burstein et al. (1973)

[a] Abbreviations: BO, bacterioopsin; BR, bacteriorhodopsin; HSA, human serum albumin; LADH, horse liver alcohol dehydrogenase; NATA, *N*-acetyltryptophanamide; subtilisin C, subtilisin Carlsberg. [b] Fluorescence yield for 80% glycerol–buffer (F_g) (pH 7) relative to 100% aqueous suspensions (F_w); 295-nm excitation.

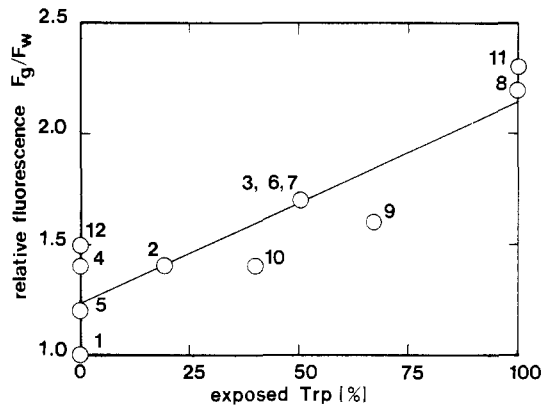

FIGURE 5: Correlation between glycerol-induced fluorescence enhancement and Trp exposure for selected proteins. Protein numbering as in Table III. Linear least-squares fit: intercept = 1.23 ± 0.09 (SD); slope = (9.09 ± 1.55) × 10^{-3}; correlation coefficient = 0.900.

excitation). A qualitatively similar phenomenon was observable with monomeric Trp and with NATA, yields attaining a limiting increase of 120% at ca. 70% v/v glycerol. The emission from a selection of nine other globular proteins was also compared in aqueous and 80% v/v glycerol–water mixtures, and the relative fluorescence quantum yields were measured (Table IV). The data are plotted against literature estimates (loc. cit.) of the percent exposure of Trp residues in these proteins in Figure 5. The data conform to a linear least-squares fit with a correlation coefficient of 0.900.

Effect of Lanthanide Ions. No significant effect on emission quantum yield or band shape for either BR or BO aqueous suspensions was observed in the presence of up to 100 μM (100 mol equiv) Tb(III) or Eu(III). This was the practical limiting concentration of lanthanide ion in this system since at this concentration an onset of turbidity occurred, presumably owing to neutralization of membrane surface charge by bound lanthanide ions. Tb(III) produced no detectable (±3%) change in quantum yields, nor was any sensitized Tb emission detectable at $\lambda > 500$ nm. With Eu(III) in the range 5–50 mol equiv, 3% (SD = 3%; $N = 6$) and 2% (SD = 3%; $N = 3$) decreases in both BR and BO quantum yields, respectively, were measured. However, no change in band shape could be detected, and spectral subtraction gave no evidence of red-shifted bands characteristic of quenching of exposed Trp residues.

Effect of Acrylamide. The quenching profiles for aqueous suspensions of BR and BO are plotted in Figure 6 where it

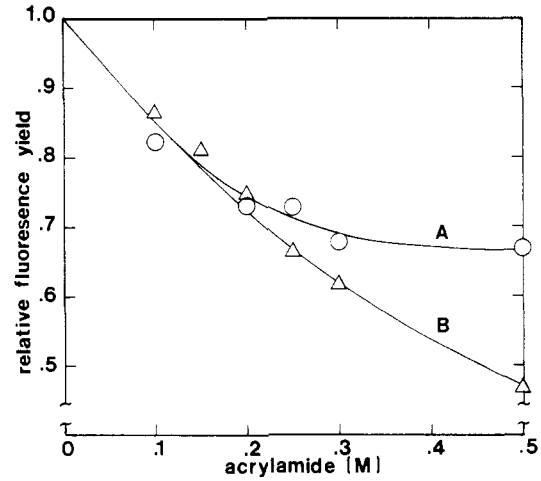

FIGURE 6: Acrylamide quenching of protein fluorescence emission: (A) bacteriorhodopsin (BR); (B) bacterioopsin (BO).

Table V: Quenching of BR and BO Fluorescence by Acrylamide

quenching parameter[a]	BR		BO	
	330 nm	360 nm	330 nm	360 nm
K (M^{-1})[b]			2.6 ± 0.3	2.3 ± 0.1
f[c]	0.82 ± 0.08	0.44 ± 0.04		
K (M^{-1})[c]	2.7 ± 0.3	7.1 ± 1.4		

[a] Calculated from plots according to eq 1 or 2; quoted error is 1 standard deviation. [b] From Stern–Volmer plots (eq 1). [c] From modified Stern–Volmer plots (eq 2).

may be seen that the relative fluorescence yields for acrylamide quenching of BR emission approach an asymptotic value more rapidly than those of BO. The data were analyzed on the basis of the Stern–Volmer relationship (eq 1) (Stern & Volmer,

$$I_0/I = 1 + K[Q] \quad (1)$$

1919) where I_0 and I are respectively the fluorescence intensities at a given wavelength in the absence and presence of quencher with concentration [Q] and K is the collisional quenching constant. While data for BO conform well to a linear plot for intensities measured at 330 and 360 nm (correlation coefficients, respectively, of 0.978 and 0.994), the data for BR exhibited distinct curvature. The latter data were replotted according to the modified Stern–Volmer relationship suggested by Lehrer (1971) (eq 2) where ΔI is the decrease

$$I_0/\Delta I = \sum[1/f_i + 1/(f_i K_i[Q])] \quad (2)$$

in fluorescence intensity produced by quencher concentration [Q] and f_i is the fraction of fluorophores accessible to the quencher with collisional quenching constant K_i. In this form, the data conform well to linear plots (correlation coefficients, respectively, of 0.997 and 0.970 for 330- and 360-nm emissions). The Stern–Volmer parameters obtained from the four plots are listed in Table V.

The heterogeneity for acrylamide quenching which is apparent from the quenching curves for different wavelengths is also demonstrated in the difference spectra obtained by subtracting the emission band in the presence of acrylamide from that of quencher-free suspensions of BR and BO (panels A and B, respectively, of Figure 7). The relative signal amplitudes for buried, surface, and exposed residues for BR are 51, 18, and 31%, respectively, and for BO, they are 47, 21, and 33%, respectively. While at this acrylamide concentration there is no net preference for the putative exposed Trp residues over the others of BR (I is identical with that for total BR residue emission), discrimination in favor of exposed residues is apparent in BO ($I_R = 0.49$).

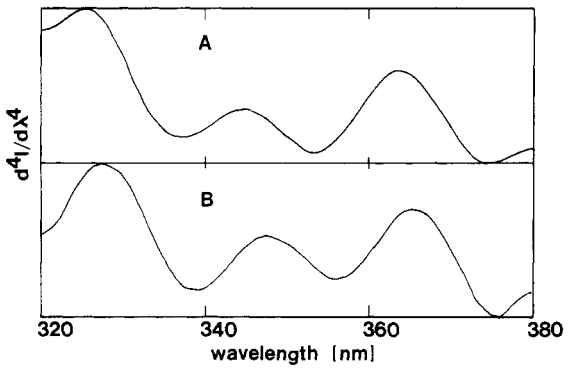

FIGURE 7: Fourth derivative of difference spectrum between, respectively, protein emission in the absence and presence of acrylamide (0.2 M); 295-nm excitation: (A) bacteriorhodopsin (BR); (B) bacterioopsin (BO).

Table VI: Distribution of Trp Emission Bands

	distribution of band intensities (%) at			rel no. of Trp residues[a]		
protein	325 nm	340 nm	360 nm	325 nm	340 nm	360 nm
BR	51	18	31	1.5	1.0	2.4
BO	54	18	28	1.9	1.0	2.5

[a] Using weighting factors of 0.40 and 0.67, respectively, for internal and surface Trp residues on the basis of the data of Privat et al. (1979).

Discussion

Primarily on the basis of the observation of large protein fluorescence bandwidths in the preliminary study of emission from aqueous suspensions of purple membrane fragments (Sherman, 1981), it was concluded that a significant proportion of Trp residues of BR are exposed to the aqueous medium. The present detailed analysis of the emission band shape supports this conclusion. The utility of fourth-derivative spectroscopy as a powerful technique for the resolution of protein absorption bands attributable to aromatic residues has been analyzed in detail by Butler (1979). We here suggest that this technique may be extended to protein emission spectra for the resolution of contributions from exposed, surface, and buried Trp residues. On the basis of fourth-derivative spectroscopic data (Figure 3) and appropriate weighting factors (Privat et al., 1979) for relative quantum yields for the three categories of Trp residues (buried, surface, and exposed), it may be estimated that exposed residues make up about half the total population of Trp fluorophores of native BR and its chromophore-free apoprotein (Table VI). A major contribution to red-shifted Trp emission, attributable to buried lipophilic residues which may be complexed to peptide carbonyls or polar side chains (Longworth, 1971), is excluded since this emission is significantly reduced in dry, lyophilized powders (W. V. Sherman and B. J. Plotkin, unpublished results).

Spectral heterogeneity in fluorescence emission of multitryptophanyl proteins has been widely used as evidence for different sites for these residues. However, as has been reviewed by Galley (1976), this phenomenon may also reflect incomplete solvent relaxation during the lifetime of the excited state. Furthermore, spectral heterogeneity may also result from different conformations (rotamers) of the alanyl side chain of even identical Trp residues of different protein molecules (Fleming et al., 1978; Szabo & Rayner, 1980). These alternative putative causes of spectral heterogeneity are explored in the present study of fourth-derivative analysis of monomolecular Trp in solvents with a range of dielectric constants (2-propanol and dioxane–water mixtures) and also in a low dielectric constant medium (pure dioxane) (Table III). While even in the latter spectral heterogeneity persists, the red-shifted band is considerably smaller than that found for Trp in BR and in BO. Clearly, therefore, the spectral properties of BR and BO cannot be exclusively attributed to phenomena cited above, since they should be retained to a similar degree in all fluid media. However, the presence of residual spectral heterogeneity in nonaqueous media shows that caution should be used in quantitative estimates of Trp microenvironments.

A wide range of studies of LADH which includes phosphorescence (Purkey & Galley, 1970), fluorescence quenching (Abdallah et al., 1978; Eftink & Ghiron, 1981; Calhoun et al., 1983), time-resolved fluorometry (Ross et al., 1981), room-temperature phosphorescence (Saviotti & Galley, 1974; Calhoun et al., 1983), and optical detection of magnetic resonance [see Kwiram & Ross (1982) and references cited therein] have led to the conclusion that of the two Trp residues in the monomer unit, one (Trp-15) is exposed and the other (Trp-314) is buried. Spectral resolution of the LADH fluorescence by fourth-derivative spectroscopy (Figure 4B) shows essentially two bands with maxima at 360 and 325 nm corresponding to exposed and buried Trp residues, respectively, with an unresolved small shoulder at ca. 340 nm. The maximum signal amplitude of the exposed fluorophore is 0.43 that of the sum of amplitudes for buried and surface fluorophores (Table III). If it is assumed that the red-shifted band represents half the Trp population of LADH, then the value for the ratio of hydrophilic to lipophilic Trp residues, which is essentially identical with that obtained for BR (Table III), supports the foregoing calculation of Trp heterogeneity in BR based on quantum yield estimates (Table VI).

Quenching by acrylamide of BR 360-nm emission, most characteristic of exposed Trp, conforms best to the modified Stern–Volmer relationship with a limiting quenchable fluorophore population of 0.44 ± 0.04 of the total (Table V). The Stern–Volmer collisional quenching rate constant, 7.1 ± 1.4 M^{-1}, is in agreement with that obtained by Eftink & Ghiron (1981) for quenching of Trp-15 in LADH (9.1 M^{-1} at 25 °C). However, the agreement between the quenchable Trp population obtained by this analysis and those estimates obtained above while very satisfying must be accepted as confirmatory only with some reservation. Thus, the fourth derivative of the difference spectrum for acrylamide quenching (Figure 7) while exhibiting a strong band at 360 nm also indicates that surface and even buried fluorophores are affected. A linear modified Stern–Volmer plot is also obtained for 330-nm emission with $f = 0.82 \pm 0.08$ and $K = 2.7 \pm 0.4$ M^{-1}. The penetration of acrylamide into lipophilic regions of the protein structure is consistent with the stochastic fluctuation model of protein structure proposed by Lakowicz & Weber (1973). In this model, quenching of buried fluorophores by a water-soluble quencher is controlled by the permeability of the protein matrix resulting from structural fluctuations that facilitate the inward diffusion of the quencher. The quenching constants for 360-nm emission intensities are typical for exposed protein Trp residues, while the lower value for lipophilic residues is typical for processes controlled by the rate of opening of channels within the protein matrix allowing access of acrylamide (Eftink & Ghiron, 1977, 1981).

The lipid composition of PM is characterized by a preponderance of negatively charged phospholipids (Eisenbach & Caplan, 1979). Thus, in the quenching studies with lanthanide ions, it is to be expected that these metal ions bind strongly to the negatively charged membrane surface. This is supported by our observation of the onset of turbidity at ca.

100 metal ion mol equiv per protein which we ascribe to neutralization of membrane surface charge. The estimated 1:10 protein to lipid composition for the membrane fragments (Eisenbach & Caplan, 1979) places the metal ion to lipid mole equivalence at ca. 10. Thus, in spite of the low quencher concentrations used in the lanthanide study—compared to those used for acrylamide—the putative surface binding of the former would be expected to result in high localized concentrations of lanthanide ions. If the foregoing analysis is correct, then the absence of significant quenching by Tb(III) or Eu(III) clearly demonstrates that the putative exposed Trp fluorophores of BR are not at the membrane surface nor are they, or the other (blue-shifted) fluorophores, within 10 Å of the surface since residues at this depth would be affected by Eu(III) which has a critical radius of 10 Å (Richardson, 1980).

The original motivation for studying solvent perturbation of fluorescence emission from BR grew out of apparent discrepancies between fluorescence lifetimes measured by one of us (Sherman, 1982) and those of Kalisky et al. (1981a). Examination of the experimental details of the latter work reveals the presence of high concentrations of sucrose in the suspending medium used to reduce turbidity and associated light-scattering artifacts. We have determined that sucrose affects the fluorescence quantum yield (unpublished results) and also the photochemical cycle lifetime (Sherman & Caplan, 1975; Eisenstein, 1982). To test whether the influence of sucrose was a nonspecific medium viscosity effect (Rice et al., 1980; Gusten & Meisner, 1983) and to avoid the poor optical clarity of sucrose in the ultraviolet, fluorescence measurements were performed with BR and with BO in glycerol–water mixtures. The enhancement of fluorescence yield observed with these proteolipid complexes appears to be a general characteristic of globular proteins with putative exposed Trp residues and also of monomeric Trp (Table IV, Figure 5). On the basis of the linear correlation for the nine proteins and monomeric Trp (Table IV), values for the proportion of emitting Trp exposed to solvent in BR and BO are obtained which are consistent with estimates based on derivative spectrofluorometry and fluorescence quenching.

To summarize the foregoing, clear evidence is presented for the exposure to water of intrasegment portions of the polypeptide chain of BR in its native conformation in the purple membrane. These portions are buried within the lipoprotein matrix. As a consequence of Trp → retinylidene energy transfer, the Trp residues responsible for fluorescence emission from native BR constitute a minority of these polypeptide residues (Kalisky et al., 1981a; Sherman, 1982). This is confirmed by the 5-fold increase in fluorescence quantum yield observed for chromophore-free BO (Table I). Thus, in BO, emission is principally representative of Trp residues which are nonfluorescent in native BR. These additional fluorophores do not significantly change the hydrophilic/lipophilic balance. Therefore, while on the basis of the BR emission data we concluded that about half the Trp residues remote from the retinylidene chromophore are hydrophilic, it also follows that only a little less than half of those close to the chromophore (within the critical distance for singlet energy transfer of 25 Å; Kalisky et al., 1981a) are also exposed to an aqueous environment. Without resorting to speculation concerning the disposition of the seven helical segments A–G (Figure 1A) with respect to sites 1–7 in the purple membrane matrix (Figure 1B), the two Trp residues in segment F to which the segment containing Lys-216 is attached by a very short linking section may be expected to be nonfluorescent in BR. These two Trp residues (Trp-182 and Trp-189) have a vertical (with respect to the membrane surfaces) separation of about 10 Å from each other and a similar lateral location on the α-helix (assuming a typical α-helix with 3.6 residues per turn and a pitch of 5.4 Å). Their proximity is such that they are either both lipophilic or both hydrophilic. In the former case, the three or four of the remaining six residues (in segments A, C, and E) which are nonfluorescent in BR (Kalisky et al., 1981a) are mostly hydrophilic. Since these residues are not deeply buried, this could indicate an intrasegment aqueous region which may not penetrate the protein to more than half its depth from the outside surface. In the latter case, however, an aqueous region penetrating more than halfway through the protein is indicated, and this could well constitute an aqueous channel for the transmembrane transport of protons. In either case, the intrasegment aqueous region is within 25 Å of the retinylidene chromophore and therefore may be expected to be intimately involved in the light-driven ion-pumping phenomenon.

There is considerable support for the separate or mutual proximity of water and of Trp and/or Tyr to the retinylidene Schiff base linkage in rhodopsins. Spectral studies have indicated that water is involved in the protonation of the Schiff base in animal rhodopsin (Rafferty & Shichi, 1981) and may also be involved in the retinylidene-binding site in BR [see Korenstein & Hess (1982) and references cited therein]. More extensive evidence exists for interaction between Trp and/or Tyr and the retinylidene chromophore in both animal rhodopsin and BR (Rafferty, 1979; Chabre & Breton, 1979; Hess & Kuschmitz, 1979; Rafferty et al., 1980; Kalisky et al., 1981b; Lemke & Oesterhelt, 1981; Rosenfeld et al., 1982). Furthermore, model protonated Schiff base pigments with striking spectral similarity to the BR α-band chromophore have been prepared by complexation of retinal with tryptophan (Ishigami et al., 1966; Mendelsohn, 1973; Johnston et al., 1982).

A proton-conducting pore through the purple membrane which involves a hydrogen-bonded chain of several Tyr residues in the intrasegment interior of BR (Figure 1B) has been proposed recently as an important component of the light-driven proton pump (Merz & Zundel, 1981, 1983). According to this proposal, contact between helical segments B, C, and E (Figure 1A) would permit a chain of six Tyr residues (counting from the cytoplasmic side of the protein, residues 150, 147, 58, 83, 65, and 79) linked by phenolate hydrogen bonds. By means of this chain, a proton flux may traverse the membrane by a Grotthus mechanism (Nagle et al., 1980). The carboxylate proton of Glu-74 forms the terminus of the chain at the membrane exterior surface while Asp-115, or Asp-212, is at the other end. The latter is also associated with the retinyldiene chromophore and with Tyr-26 at the cytoplasmic surface. Assuming a protein structure composed of normal α-helical segments (see above), this arrangement would require that Trp-10, Trp-80, Trp-137, and Trp-138 be directed away from the putative intrasegment proton-conducting pore while on the same basis Trp-12 and Trp-86 would be within a 60° lateral sector common to the Tyr residues of their respective helical segments. These two Trp residues, and possibly also Trp-182 and/or Trp-189, would thus be in contact with the proton-conducting pore. Such a pore may be considered to possess a hydrophilic character with an icelike structure, and although the presence of bound water molecules is not essential, they are not excluded (Nagle et al., 1980). Thus, interaction with this pore may be responsible for a red shift in from two to four of the eight potential Trp fluorophores of BO. Grouping segments B, C, E, and F close to each other, as required by the pore model, places Trp-12 and Trp-86

within the critical distance for singlet energy transfer to the retinylidene chromophore in BR, and since F is also joined to G by only a short intersegment linking section, the same is true for Trp-182 and Trp-189. This leaves Trp-10, Trp-80, Trp-137, and Trp-138 as the prinicipal potential fluorophores of BR. All of these are near the membrane surface, but the absence of any significant quenching of BR fluorescence by Eu(III) shows that they are sufficiently buried as not to exhibit typically hydrophilic emission. However, Trp-137 is in the same lateral sector of segment E as Tyr-133 and Arg-134 and comes within a possible locus of the ϵ-amino group of Lys-129 of adjacent segment D (this orientation of segment D with respect to segment E is required if Asp-115 participates in the proton-conduction pore). Hydrogen bonding between these three or four polar residues may constitute a polar environment for Trp-137 (Longworth, 1971) and be responsible for part of the red-shifted component of Trp emission from BR.

Added in Proof

It has been drawn to our attention (C. R. Coan, personal communication) that on the basis of the ability of Trp to form a charge-transfer complex with 1-methylnicotinamide chloride, 0.5 is a better estimate of the Trp residues that are exposed in native trypsin (Deranleau et al., 1975). This improves the fit of this protein (datum point 12) in the glycerol-enhancement correlation (Figure 5).

Registry No. Trp, 73-22-3; NATA, 10346-41-5; LADH, 9031-72-5; acrylamide, 79-06-1; glycerol, 56-81-5.

References

Abdallah, M. A., Biellman, J. F., Wiget, P., Joppich-Kuhn, R., & Luisi, P. L. (1978) *Eur. J. Biochem. 89*, 397–405.

Bayley, H., Huang, K. S., Radhakrishnan, R., Ross, A. H., Takagaki, Y., & Khorana, H. G. (1981) *Proc. Natl. Acad. Sci. U.S.A. 78*, 2225–2229.

Becher, B., & Cassim, J. Y. (1975) *Prep. Biochem. 5*, 161–178.

Becher, B., Tokunaga, F., & Ebrey, T. G. (1978) *Biochemistry 17*, 2293–2300.

Bell, K. L., & Brenner, H. C. (1982) *Biochemistry 21*, 799–804.

Blaurock, A. E. (1975) *J. Mol. Biol. 93*, 139–158.

Burstein, E. A., Vendenkina, N. S., & Irkova, M. N. (1973) *Photochem. Photobiol. 18*, 263–279.

Butler, W. L. (1979) *Methods Enzymol. 56*, 501–515.

Cahill, J. E. (1979) *Am. Lab. (Fairfield, Conn.) 11*, 79–85.

Cahill, J. E., & Padera, F. G. (1980) *Am. Lab. (Fairfield, Conn.) 12*, 101–112.

Calhoun, D. B., Vanderkooi, J. M., & Englander, S. W. (1983) *Biochemistry 22*, 1526–1532.

Chabre, M., & Breton, J. (1979) *Photochem. Photobiol. 30*, 295–299.

Deranleau, D. A., Hinman, L. M., & Coan, C. R. (1975) *J. Mol. Biol. 94*, 567–582.

Donovan, J. W. (1969) in *Physical Principles and Techniques of Protein Chemistry* (Leach, S. J., Ed.) pp 101–170, Academic Press, New York.

Downer, N. W., & Englander, S. W. (1977) *J. Biol. Chem. 25*, 8092–8100.

Eftink, M. R., & Ghiron, C. A. (1977) *Biochemistry 16*, 5546–5551.

Eftink, M. R., & Ghiron, C. A. (1981) *Anal. Biochem. 114*, 199–227.

Eisenstein, L. (1982) *Methods Enzymol. 88*, 297–305.

Engelman, D. M., Henderson, R., McLachlan, A. D., & Wallace, B. A. (1980) *Proc. Natl. Acad. Sci. U.S.A. 77*, 2023–2027.

Fleming, G. R., Morris, J. M., Robbins, R. J., Woolfe, G. J., Thistlewaite, P. J., & Robinson, G. W. (1978) *Proc. Natl. Acad. Sci. U.S.A. 75*, 4642–4656.

Galley, W. C. (1976) in *Biochemical Fluorescence: Concepts* (Chen, R. F., & Edelhoch, H., Eds.) Vol. 2, pp 409–439, Marcel Dekker, New York.

Handbook of Physics and Chemistry (1980) 60th ed., CRC Press, Boca Raton, FL.

Henderson, R., & Unwin, P. T. (1975) *Nature (London) 237*, 28–32.

Hess, B., & Kuschmitz, D. (1979) *FEBS Lett. 100*, 334–340.

Honig, B. (1982) *Curr. Top. Membr. Transp. 16*, 371–382.

Huang, K. S., Radhakrishnan, R., Bayley, H., & Khorana, H. G. (1982) *J. Biol. Chem. 257*, 13616–13623.

Ishigami, M., Maeda, Y., & Mishima, M. (1966) *Biochim. Biophys. Acta 112*, 372–375.

Johnston, D. S., Clark, A. D., Kemp, C. M., & Chapman, D. (1982) *Biochim. Biophys. Acta 679*, 400–403.

Kalisky, O., Feitelson, J., & Ottolenghi, M. (1981a) *Biochemistry 20*, 205–209.

Kalisky, O., Ottolenghi, M., Honig, B., & Korenstein, R. (1981b) *Biochemistry 20*, 649–655.

Khorana, H. G., Gerber, G. E., Herlihy, W. C., Gray, C. P., Anderegg, R. J., Nehei, K., & Biemann, K. (1979) *Proc. Natl. Acad. Sci. U.S.A. 76*, 5046–5050.

Korenstein, R., & Hess, B. (1982) *Methods Enzymol. 88*, 180–201.

Kwiram, A. L., & Ross, J. B. A. (1982) *Annu. Rev. Biophys. Bioeng. 11*, 223–249.

Lakowicz, J. R., & Weber, G. (1973) *Biochemistry 12*, 4171–4179.

Lehrer, S. S. (1971) *Biochemistry 10*, 3254–3263.

Lemke, H. D., & Oesterhelt, D. (1981) *Eur. J. Biochem. 115*, 595–604.

Longworth, J. W. (1971) in *Excited States of Proteins and Nucleic Acids* (Steiner, R. F., & Weinryb, I., Eds.) Chapter 6, Plenum Press, New York.

Mendelsohn, R. (1973) *Nature (London) 243*, 22–24.

Merz, H., & Zundel, G. (1981) *Biochem. Biophys. Res. Commun. 101*, 540–546.

Merz, H., & Zundel, G. (1983) *Chem. Phys. Lett. 95*, 529–532.

Montal, M., Davszon, A., & Trissl, H. W. (1977) *Nature (London) 267*, 221–225.

Nagle, J. F., Mille, M., & Morowitz, H. J. (1980) *J. Chem. Phys. 72*, 3959–3971.

Oesterhelt, D., & Stoeckenius, W. (1971) *Nature (London), New Biol. 233*, 149–152.

Oesterhelt, D., & Stoeckenius, W. (1974) *Methods Enzymol. 31*, 667–678.

O'Haver, T. C., & Green, G. L. (1976) *Anal. Chem. 48*, 312–318.

Ottolenghi, M. (1980) *Adv. Photochem. 12*, 97–200.

Ovchinnikov, Y. A., Abdulaev, N. G., Feigina, M. Y., Kiselev, A. V., & Lobanov, N. A. (1979) *FEBS Lett. 100*, 219–224.

Privat, J. P., Wahl, P., & Auchet, J. C. (1979) *Biophys. Chem. 9*, 223–233.

Purkey, R. M., & Galley, W. C. (1970) *Biochemistry 9*, 3569–3575.

Rafferty, C. N. (1979) *Photochem. Photobiol. 29*, 109–120.

Rafferty, C. N., & Shichi, H. (1981) *Photochem. Photobiol. 33*, 229–234.

Rafferty, C. N., Muellenberg, C. G., & Shichi, H. (1980) *Biochemistry 19*, 2145–2151.

Richardson, F. S. (1982) *Chem. Rev. 82*, 541–552.

Rogan, P. K., & Zaccai, G. (1981) *J. Mol. Biol. 145*, 281-283.
Rosenfeld, V., Goldberg, R., Gilon, C., & Ottolenghi, M. (1982) *Photochem. Photobiol. 36*, 197-201.
Ross, J. B., Schmidt, C. J., & Brand, L. (1981) *Biochemistry 20*, 4369-4377.
Rousslang, K. W., Thomasson, J. M., Ross, J. B., & Kwiram, A. L. (1979) *Biochemistry 18*, 2296-2300.
Saviotti, M. L., & Galley, W. C. (1974) *Proc. Natl. Acad. Sci. U.S.A. 71*, 4154-4158.
Savitsky, A., & Golay, M. J. (1964) *Anal. Chem. 36*, 1627-1630.
Sherman, W. V. (1981) *Photochem. Photobiol. 33*, 367-371.
Sherman, W. V. (1982) *Photochem. Photobiol. 36*, 463-469.
Sherman, W. V., & Caplan, S. R. (1975) *Nature (London) 258*, 766-768.
Sherman, W. V., Slifkin, M. A., & Caplan, S. R. (1975) *Biochim. Biophys. Acta 423*, 238-248.
Stern, O., & Volmer, M. (1919) *Phys. Z. 20*, 183-188.
Stoeckenius, W., & Bogomolni, R. A. (1982) *Annu. Rev. Biochem. 51*, 587-616.
Szabo, A. G., & Rayner, D. M. (1980) *J. Am. Chem. Soc. 102*, 554-563.
Tokunaga, F., & Ebrey, T. (1978) *Biochemistry 17*, 1915-1922.
Williams, J. F. (1981) Perkin-Elmer Technical Note 2009, Perkin-Elmer Corp., Norwalk, CT.

Carboxylation of Pyruvate and Acetyl Coenzyme A by Reversal of the Na^+ Pumps Oxaloacetate Decarboxylase and Methylmalonyl-CoA Decarboxylase†

Peter Dimroth* and Wilhelm Hilpert

ABSTRACT: Proteoliposomes reconstituted by detergent dialysis from purified oxaloacetate decarboxylase and phospholipids catalyzed an oxaloacetate-$^{14}CO_2$ exchange. Similarly prepared proteoliposomes containing methylmalonyl-CoA decarboxylase catalyzed the exchange between malonyl-CoA and $^{14}CO_2$. These exchange reactions were completely dependent on the Na^+ ion gradients established during decarboxylation of part of the substrates since no exchange took place in the presence of the Na^+ carrier monensin. After a large Na^+ concentration gradient $Na_{in}^+ > Na_{out}^+$ was applied to methylmalonyl-CoA decarboxylase containing proteoliposomes, acetyl coenzyme A (acetyl-CoA) was carboxylated to malonyl-CoA which was trapped with fatty acid synthetase. In the absence of a Na^+ gradient, no acetyl-CoA carboxylation occurred. When oxaloacetate decarboxylase and methylmalonyl-CoA decarboxylase were simultaneously incorporated into proteoliposomes, a transcarboxylase system was constructed. Upon decarboxylation of oxaloacetate to pyruvate, acetyl-CoA was carboxylated to malonyl-CoA and vice versa. These transcarboxylations are mediated by a Na^+ circuit since dissipation of the Na^+ gradient with monensin also abolished the transcarboxylation reactions. Disruption of the membrane potential with valinomycin or carbonyl cyanide *p*-(trifluoromethoxy)-phenylhydrazone severely reduced the rate of oxaloacetate decarboxylation dependent acetyl-CoA carboxylation, in accord with the electrogenic properties of the Na^+ pumps. These Na^+ pumps therefore act as reversible vectorial catalysts either by creating electrochemical Na^+ gradients upon decarboxylation or by CO_2 fixation to yield carboxylic acids at the expense of an already existing Na^+ gradient. This type of CO_2 fixation is new and basically different from the classical carboxylation reactions which require ATP hydrolysis to overcome the energetically unfavorable metabolic processes. The stoichiometry between Na^+ transport and malonyl-CoA decarboxylation was 2:1 in the initial phase but decreased after a Na^+ concentration gradient had developed over the vesicular membrane.

The free energy of decarboxylation reactions is used by certain anaerobic bacteria to drive the active transport of Na^+ ions through the cell membrane (Dimroth, 1982a). Three enzymes have been recognized to perform this kind of energy transduction, i.e., oxaloacetate decarboxylase (Dimroth, 1980), methylmalonyl-CoA decarboxylase (Hilpert & Dimroth, 1982) and glutaconyl-CoA decarboxylase (Buckel & Semmler, 1982). These sodium transport decarboxylases have a number of properties in common, e.g., binding to the membrane, specific activation by Na^+ ions, and the prosthetic group biotin. Incorporation of purified oxaloacetate decarboxylase into phospholipid vesicles led to the reconstitution of Na^+ transport activity (Dimroth, 1981). Subsequently, the two other Na^+ pumps were reconstituted in use of the same reconstitution procedure (Hilpert & Dimroth, 1984; Buckel & Semmler, 1983).

Most of our knowledge on the mechanism of the Na^+ pumps has come from studies of oxaloacetate decarboxylase. The first step is a transfer of the carboxyl group from oxaloacetate to the enzyme-bound biotin (Dimroth, 1982c). This reaction is catalyzed by a distinct carboxyltransferase subunit which is a soluble protein (Dimroth & Thomer, 1983) analogous to the carboxyltransferase subunits of biotin-dependent carboxylases. The carboxyl transfer is completely independent from the presence of Na^+ ions and is freely reversible as shown by the exchange of radioactivity between [1-^{14}C]pyruvate and oxaloacetate (Dimroth, 1982c; Dimroth & Thomer, 1983). The next step is a Na^+-dependent decarboxylation of the carboxybiotin enzyme intermediate, and this apparently makes the overall decarboxylation process irreversible. So far, the reversibility has only been studied with the soluble enzymes, i.e.,

† From the Institut für Physiologische Chemie der Technischen Universität München, 8000 München 40, West Germany. *Received March 22, 1984.* This work was supported by the Deutsche Forschungsgemeinschaft and the Fonds der Chemischen Industrie.

0006-2960/84/0423-5360$01.50/0